

# One Collision—Two Substituents: Gas-Phase Preparation of Xylenes under Single-Collision Conditions

Iakov A. Medvedkov, Anatoliy A. Nikolayev, Chao He, Zhenghai Yang, Alexander M. Mebel,\* and Ralf I. Kaiser\*

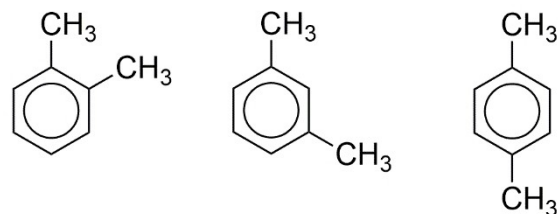
**Abstract:** The fundamental reaction pathways to the simplest dialkylsubstituted aromatics—xylenes ( $C_6H_4(CH_3)_2$ )—in high-temperature combustion flames and in low-temperature extraterrestrial environments are still unknown, but critical to understand the chemistry and molecular mass growth processes in these extreme environments. Exploiting crossed molecular beam experiments augmented by state-of-the-art electronic structure and statistical calculations, this study uncovers a previously elusive, facile gas-phase synthesis of xylenes through an isomer-selective reaction of 1-propynyl (methylethynyl,  $CH_3CC$ ) with 2-methyl-1,3-butadiene (isoprene,  $C_5H_8$ ). The reaction dynamics are driven by a barrierless addition of the radical to the diene moiety of 2-methyl-1,3-butadiene followed by extensive isomerization (hydrogen shifts, cyclization) prior to unimolecular decomposition accompanied by aromatization via atomic hydrogen loss. This overall exoergic reaction affords a preparation of xylenes not only in high-temperature environments such as in combustion flames and around circumstellar envelopes of carbon-rich Asymptotic Giant Branch (AGB) stars, but also in low-temperature cold molecular clouds (10 K) and in hydrocarbon-rich atmospheres of planets and their moons such as Triton and Titan. Our study established a hitherto unknown gas-phase route to xylenes and potentially more complex, disubstituted benzenes via a single collision event highlighting the significance of an alkyl-substituted ethynyl-mediated preparation of aromatic molecules in our Universe.

## Introduction

Since the very first isolation of xylenes—*ortho*-(*o*), *meta*-(*m*), and *para*-(*p*) dimethyl substituted benzenes (**1–3**;  $C_6H_4(CH_3)_2$ ; Scheme 1)—by Auguste Cahours as constituents of wood tar in 1850,<sup>[1]</sup> the gas-phase formation mechanisms and role of distinct xylene isomers in combustion flames and in extraterrestrial environments (cold molecular clouds, circumstellar envelopes) have attracted extensive interest from the combustion chemistry,<sup>[2–5]</sup> astrochemistry,<sup>[2,6,7]</sup> industrial chemistry,<sup>[8]</sup> and physical organic chemistry communities.<sup>[9,10]</sup> These isomers are the simplest representatives of dialkyl-substituted benzenes with methyl groups augmenting the reactivity toward electrophile ( $S_EAr$ )<sup>[11,12]</sup> and radical substitution ( $S_RAr$ )<sup>[11]</sup> compared to benzene.

In methyl-substituted benzenes, the carbon-hydrogen bond of the methyl moiety is considerably weaker by  $100\text{ kJ mol}^{-1}$  compared to the ‘aromatic’ carbon-hydrogen bond.<sup>[13–17]</sup> A homolytic carbon-hydrogen bond cleavage at the  $sp^3$ -hybridized carbon atom results in highly stable xylyl (methylbenzyl) radicals.<sup>[4,18]</sup> This enhanced stability can be rationalized in terms of a delocalization of the radical center with the  $\pi$ -system of the benzene ring allowing four resonance structures. These resonance-stabilized free radicals (RSFRs) are contemplated as vital building blocks in molecular mass growth processes of polycyclic aromatic hydrocarbons (PAHs) eventually leading to carbonaceous nanoparticles (soot, dust) via five-membered ringed aromatics<sup>[13,19,20,2]</sup> in combustion systems and in deep space.<sup>[21–26]</sup> Traditionally, in combustion models of sooting hydrocarbon flames such as of benzene suggest that xylenes can be synthesized in the gas phase via the reaction of toluene ( $C_6H_5(CH_3)$ ) with a methyl radical ( $CH_3$ ) passing a

[\*] Dr. I. A. Medvedkov, Dr. C. He0000-0001-9351-5684, Dr. Z. Yang, Prof. Dr. R. I. Kaiser  
 Department of Chemistry, University of Hawai'i at Manoa  
 Honolulu, HI 96822 (USA)  
 E-mail: ralfk@hawaii.edu  
 Homepage: 0000-0001-9351-5684  
 A. A. Nikolayev  
 Samara National Research University  
 Samara 443086 (Russia)  
 Prof. Dr. A. M. Mebel  
 Department of Chemistry and Biochemistry, Florida International University  
 Miami, FL 33199 (USA)  
 E-mail: mebela@fiu.edu



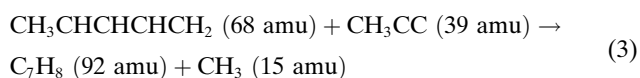
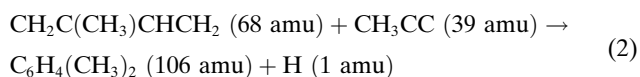
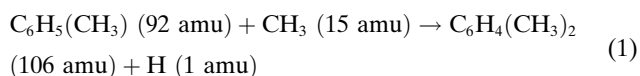
1,2-dimethylbenzene (*ortho*-xylene)    1,3-dimethylbenzene (*meta*-xylene)    1,4-dimethylbenzene (*para*-xylene)

**Scheme 1.** Structures of xylene isomers.

significant barrier to reaction of  $38 \text{ kJ mol}^{-1}$ <sup>[27]</sup> via a radical substitution mechanism (reaction (1)).

The inherent entrance barrier efficiently blocks the formation of xylene isomers in low-temperature environments such as in cold molecular clouds (10 K) and in hydrocarbon rich atmospheres of planets and their moons such as Titan (94 K). Therefore, fundamental reaction pathways to xylenes in low temperature extraterrestrial environments are still not fully untangled. The non-resonantly stabilized 1-propynyl radical ( $\text{CH}_3\text{CC}$ )—a highly reactive high energy isomer of the resonantly stabilized propargyl radical ( $\text{H}_2\text{CCCH}$ ), has attracted considerable attention for its role in molecular mass growth processes in carbon-rich extraterrestrial environments.<sup>[28–36]</sup> The high reactivity and addition of the 1-propynyl radical to double and triple bonds of hydrocarbons provide barrier-less pathways accessing toluene<sup>[29]</sup> along with hydrogen-deficient hydrocarbons<sup>[28–33]</sup> accessible even at low temperatures (10 K).

Herein, we report a facile gas-phase formation of xylene isomers via the barrierless reaction of the 1-propynyl radical ( $\text{CH}_3\text{CC}$ ;  $\text{X}^2\text{A}_1$ ) with 2-methyl-1,3-butadiene (isoprene;  $\text{X}^1\text{A}'$ ;  $\text{C}_5\text{H}_8$ ) effectively incorporating two methyl groups into a benzene molecule via a single collision event from two acyclic precursor molecules (reaction (2)). This system is also appealing from the viewpoint of the physical organic chemistry community since it reflects a prototype reaction to elucidate the preparation of a disubstituted aromatic molecule initiated by radical addition along with successive isomerization involving ring closure and hydrogen shifts, in which both methyl substituents act as spectators and are piggybacked by the reactants. Since the reaction of the 1,3-pentadiene ( $\text{X}^1\text{A}'$ ;  $\text{C}_5\text{H}_8$ ) isomer does not lead to xylenes, this investigation also allows us to trace the influence of the position of the methyl group in distinct  $\text{C}_5\text{H}_8$  isomers on the reaction dynamics thus revealing an isomer-selective stereochemistry at the molecular level. Considering that xylenes have been detected on comet 67P/Churyumov-Gerasimenko<sup>[37]</sup> and in meteorites such as in Murchison (CM2),<sup>[6,7,38]</sup> our combined experimental and computational study also provide plausible pathways to xylenes in our Universe.



## Results and Discussion

### Laboratory Frame

Reactive scattering signal of the bimolecular gas-phase reactions of the 1-propynyl radical ( $\text{CH}_3\text{CC}$ ;  $\text{X}^2\text{A}_1$ ; 39 amu)

with 2-methyl-1,3-butadiene ( $\text{CH}_2\text{C}(\text{CH}_3)\text{CHCH}_2$ ;  $\text{X}^1\text{A}'$ ; 68 amu) (reaction (2)) was searched for and observed at  $m/z = 91$  ( $\text{C}_7\text{H}_7^+$ ) and  $m/z = 106$  ( $\text{C}_8\text{H}_{10}^+$ ). The time-of-flight (TOF) spectra at  $m/z = 106$  and 91 were superimposable after scaling indicating that signal at  $m/z = 91$  originated from dissociative electron impact fragmentation of the  $\text{C}_8\text{H}_{10}$  neutral product in the electron impact ionizer of the detector (Figure S2a). These findings are in sharp contrast to the reaction of the 1-propynyl radical ( $\text{CH}_3\text{CC}$ ;  $\text{X}^2\text{A}_1$ ; 39 amu) with the 1,3-pentadiene ( $\text{CH}_3\text{CHCHCHCH}_2$ ;  $\text{X}^1\text{A}'$ ; 68 amu) isomer (reaction (3)). Here, there was no signal observable at  $m/z = 106$ ; TOFs could only be collected at  $m/z = 92$  and 91; these TOFs were superimposable after scaling (Figure S2b, c) documenting dissociative electron impact ionization of the neutral product ( $\text{C}_7\text{H}_8$ ; 92 amu) in the ionizer. For both systems, the best signal-to-noise ratio was at  $m/z = 91$ ; therefore, TOF spectra and the laboratory angular distributions (LAD) were recorded at  $m/z = 91$  (Figure 1). The best-fit LAD for the reaction of 1-propynyl with 2-methyl-1,3-butadiene (Figure 1a) spans at least  $35^\circ$  and reflects a forward-backward symmetry with respect to the center-of-mass (CM) angle of  $35.4 \pm 1.2^\circ$ . This finding proposes that the reaction involves indirect reaction dynamics through  $\text{C}_8\text{H}_{11}$  complex(es), which then undergo unimolecular decomposition through the emission of atomic hydrogen (reaction (2)). However, for the 1-propynyl/1,3-pentadiene system, the LAD depicts a higher flux in the backward hemisphere with respect to the CM angle of  $35.9 \pm 0.9^\circ$  (Figure 1b). These raw data alone provide evidence that this reaction proceeds through rather short-lived  $\text{C}_8\text{H}_{11}$  intermediates that emits a methyl radical (reaction (3)) documenting distinct exit channels in the reactions of the 1-propynyl radical with the 2-methyl-1,3-butadiene and 1,3-pentadiene isomers forming  $\text{C}_8\text{H}_{10}$  (reaction (2)) and  $\text{C}_7\text{H}_8$  isomers (reaction (3)), respectively.

### Center-of-Mass Frame

The laboratory data afford persuasive testimony for the 1-propynyl versus atomic hydrogen (reaction (2)) and methyl (reaction (3)) exchange pathways. To unravel the underlying reaction mechanism(s) and the isomer(s) formed, the laboratory data (TOF, LAD) are converted into the center-of-mass reference frame exploiting a forward-convolution routine; this procedure generates the center-of-mass translational energy ( $\text{P}(\text{E}_T)$ ) and angular ( $\text{T}(\theta)$ ) flux distribution (Figure 2).<sup>[39–46]</sup> These functions can then be exploited for the extraction of the reactive differential cross section  $\text{I}(\theta, u) \sim \text{P}(u) \times \text{T}(\theta)$ , which reports the flux as a function of the CM scattering angle  $\theta$  and velocity  $u$ ; this distribution essentially represents an overall image of the outcome of the reaction on the microscopic scale (Figure 2). First, the center-of-mass translational energy ( $\text{P}(\text{E}_T)$ ) distributions provide a valuable tool to expose the nature of the product isomer(s) formed. Here, the derived  $\text{P}(\text{E}_T)$  distributions exhibit maximum translational energy releases ( $\text{E}_{\text{max}}$ ) of  $393 \pm 28$  and  $188 \pm 37 \text{ kJ mol}^{-1}$  for the 1-propynyl/2-methyl-1,3-butadiene and 1-propynyl/1,3-pentadiene systems, re-

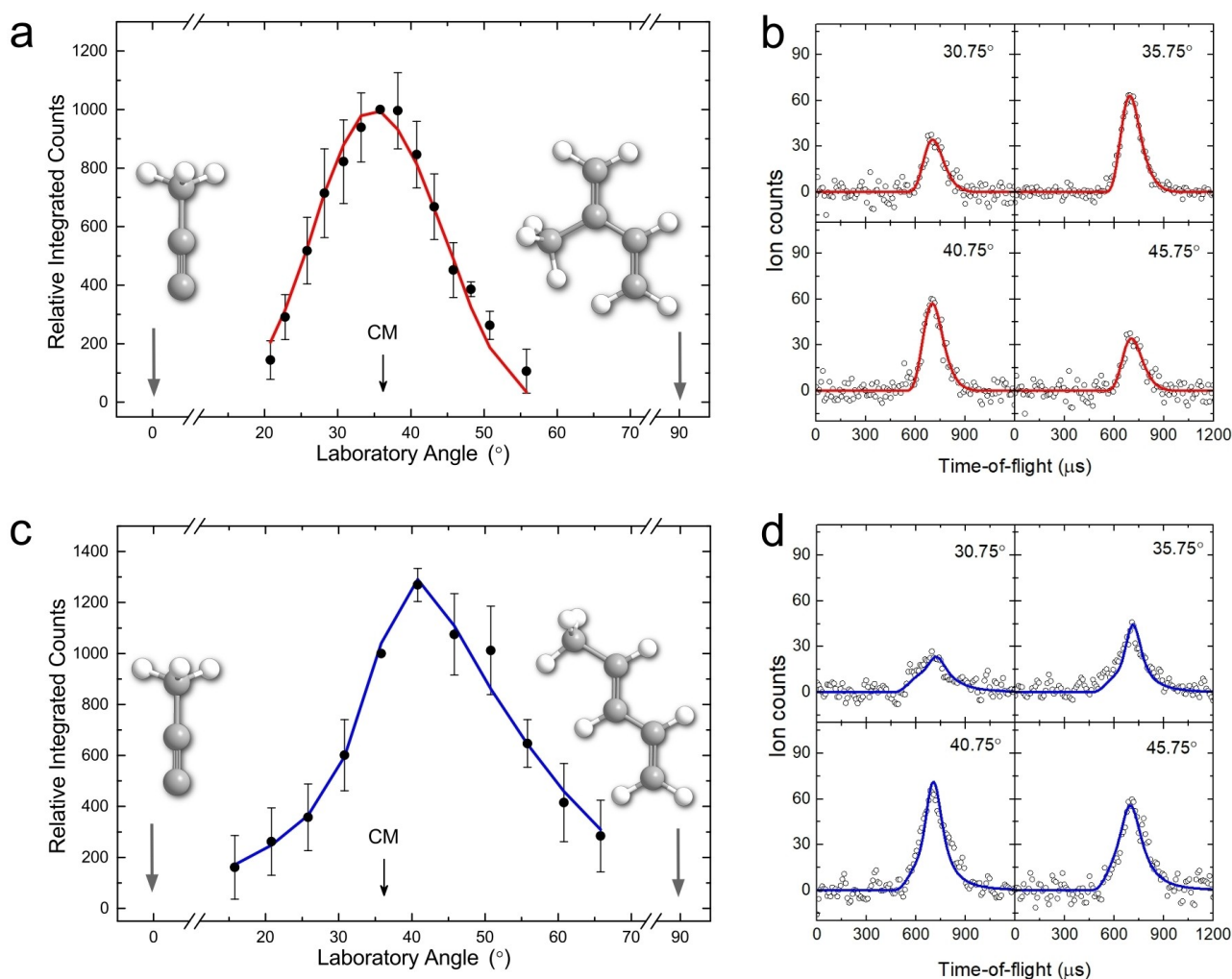


**Figure 1.** (a) Laboratory angular distribution and (b) time-of-flight (TOF) spectra recorded at  $m/z=91$  for the reaction of the 1-propynyl radical with 2-methyl-1,3-butadiene at a collision energy of  $43 \pm 2 \text{ kJ mol}^{-1}$ . (c) Laboratory angular distribution and (d) time-of-flight (TOF) spectra recorded at  $m/z=91$  for the reaction of the 1-propynyl radical with 1,3-pentadiene at a collision energy of  $43 \pm 2 \text{ kJ mol}^{-1}$ . The circles represent the experimental data and the solid lines the best fits.

spectively. Energy conservation dictates that for those molecules born without internal excitation,  $E_{\text{max}}$  is the sum of the collision energy ( $E_{\text{C}}$ ) plus the reaction energy. Therefore, reaction energies were determined to be  $-350 \pm 30 \text{ kJ mol}^{-1}$  and  $-145 \pm 39 \text{ kJ mol}^{-1}$  for reactions (2) and (3), respectively. Further, the distribution maxima of the  $P(E_{\text{T}})$  provide valuable information on the exit transition state(s) in the unimolecular decomposition of the  $\text{C}_8\text{H}_{10}$  doublet radical intermediates. Distribution maxima peak away from zero translational energy ( $61 \pm 4 \text{ kJ mol}^{-1}$ ; 1-propynyl/2-methyl-1,3-butadiene) and close to zero translational energy ( $5 \pm 1 \text{ kJ mol}^{-1}$ ; 1-propynyl/2-methyl-1,3-butadiene) indicating tight and loose exit transition states, i.e. a unimolecular fragmentation of the reaction intermediate(s) involving a significant reorganization of the electron density (reaction (2)) and a simple bond rupture process (reaction (3)).<sup>[42,43]</sup> Second, the  $T(\theta)$  distributions contain additional information on the underlying reaction dynamics. The 1-propynyl/2-methyl-1,3-butadiene system reveals non-zero flux at all

angles; the distribution also reveals a forward-backward symmetry with respect to  $90^\circ$ ; this finding suggests an indirect reaction mechanism involving long-lived  $\text{C}_8\text{H}_{11}$  intermediate(s) that have a life-time longer than their rotational period.<sup>[39]</sup> The flux minimum at  $90^\circ$  proposes geometrical constraints with the  $\text{C}_8\text{H}_{11}$  complex emitting a hydrogen atom within the rotational plane of the decomposing complex. On the other hand, for the reaction of 1-propynyl radical with 1,3-pentadiene, the center-of-mass angular flux distribution of the methyl elimination pathway depicts a pronounced backward scattering with respect to the 1-propynyl radical beam. This proposed that at least one reaction channel proceeds via backward scattering through a rebound mechanism<sup>[40,41,44]</sup> and/or an extremely short-lived  $\text{C}_8\text{H}_{11}$  reaction intermediate ejecting the methyl radical.

Our experimental data reveal distinct mechanisms upon reactions of both  $\text{C}_5\text{H}_8$  isomers with the 1-propynyl radical both in terms of the exit channels (hydrogen versus methyl group loss) and dynamics (long lived versus short-lived/

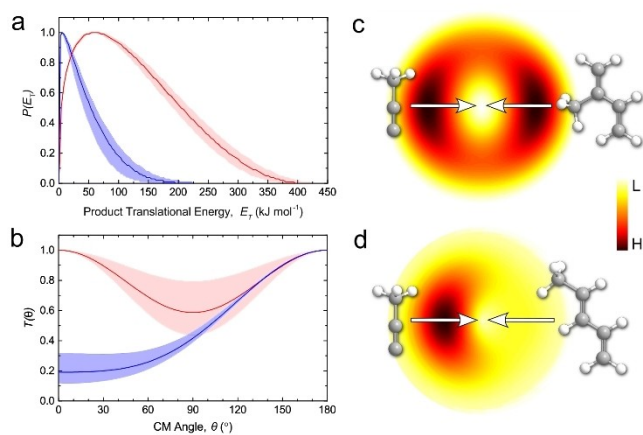


**Figure 2.** (a) Center-of-mass translational energy ( $P(ET)$ ) and (b) angular distributions ( $T(\theta)$ ) for the reaction of the 1-propynyl radical with isoprene (red) and 1,3-pentadiene (blue). Solid lines represent the best fit, while shaded areas indicate the error limits. For the  $T(\theta)$ , the direction of the 1-propynyl beam is defined as  $0^\circ$  and of the closed shell hydrocarbon beams (2-methyl-1,3-butadiene, 1,3-pentadiene) as  $180^\circ$ . (c and d) Corresponding flux contour maps for the reactions of the 1-propynyl radical with 2-methyl-1,3-butadiene (c) and 1,3-pentadiene (d).

rebound). To shed a light on these findings, the experimental results are augmented by electronic structure and statistical calculations to infer the nascent product isomer(s) and to elucidate the underlying reaction dynamics. The full potential energy surfaces (PES) (Figure S3–S16) along with results of statistical (Rice–Ramsperger–Kassel–Marcus theory method; RRKM) calculations (Table S1–S10) are compiled in the Supporting Information. These computations were conducted at a level of theory providing accuracies of the energies of the products, intermediates, and transition states with an accuracy of  $\pm 5 \text{ kJ mol}^{-1}$ ,<sup>[47,48]</sup> bond lengths and bond angles are provided within accuracies of  $\pm 0.01 \text{ \AA}$  and  $1^\circ$ , respectively.

### 1-Propynyl / 2-Methyl-1,3-Butadiene System

The bimolecular reaction of the 1-propynyl radical with 2-methyl-1,3-butadiene (isoprene) is very complex (Figure 3). Our calculations identified nine cyclic and acyclic  $\text{C}_8\text{H}_{10}$  product isomers (**p1–p9**, Figures 3) accessed via atomic hydrogen loss. In detail, the 1-propynyl radical can add barrierlessly to any of the four chemically non-equivalent carbon atoms of 2-methyl-1,3-butadiene with its radical center located at the acetylenic, terminal carbon to the  $\text{C1}=\text{C2}$  or  $\text{C3}=\text{C4}$  double bonds (Figure 3). These additions access four doublet radical intermediates **i1**, **i3**, **i9**, and **i11** stabilized by up to 217, 273, 206, and  $281 \text{ kJ mol}^{-1}$ , respectively, relative to the separated reactants. Intermediates **i1** and **i9** isomerize rapidly via ring closure through substituted cyclopropanyl radical intermediates **i2** and **i10**, followed by the ring re-opening eventually accessing **i3** and **i11** respectively. These radicals can be classified as substituted resonantly stabilized allylic radicals and they can

further undergo atomic hydrogen losses to **p4/p5** (from **i3**) or **p7/p8** (from **p11**) or proceed through a series of transformations involving, e.g., cis/trans isomerization and hydrogen shifts terminated by atomic hydrogen losses yielding acyclic products **p4** and **p7–p9** in overall exoergic reactions (from  $-94$  to  $-125 \text{ kJ mol}^{-1}$ ). The electronic structure calculations also identified reaction pathways to four cyclic reaction products: *m*-xylene (**p1**), *p*-xylene (**p2**), 1,5-dimethylenecyclohexa-1,3-diene (**p3**), and 2,5-dimethylenecyclohexa-1,3-diene (**p6**). The aromatic xylenes (**p1/p2**) are thermodynamically more stable by up to  $130 \text{ kJ mol}^{-1}$  compared to the substituted methylenecyclohexadiene products (**p3/p6**). To access **p1/p2**, the allylic intermediates **i3/i11** isomerize to **i4/i12** though rotation around the carbon-carbon bond followed by cyclization to six-membered ring carbene intermediates **i6/i17**. Here, hydrogen atom shifts to the carbene carbon atoms form low-energy intermediates **i7/i18** and/or **i8/i19**. Intermediates **i7/i18** can only fragment to **p3/p6**, while **i8/i19** offers two distinct atomic hydrogen loss exit channels to **p3/p6** and **p1**. Which of these pathways dominate? The crossed molecular beams approach has the unique advantage of extracting the nature of the isomer(s) formed by comparing the experimentally determined reaction energies with the computed reaction energies for distinct isomers. The experimentally derived reaction energy of  $-350 \pm 30 \text{ kJ mol}^{-1}$  nicely accounts for the formation of *m*- (**p1**;  $-366 \text{ kJ mol}^{-1}$ ) and *p*-xylene (**p2**;  $-367 \text{ kJ mol}^{-1}$ ) isomers under our experimental conditions via tight exit transition states located 16 to  $21 \text{ kJ mol}^{-1}$  above the separated products through overall indirect scattering dynamics. Thermodynamically unfavorable products **p3–p9** might be masked in the lower energy section of the CM translational energy distribution (Figure 2a). Our statistical (RRKM) calculation reveal that the atomic hydrogen loss channel dominates, while methyl elimination does not play a significant role (Table S2–S7, Figure S2–S7). The formation of acyclic isomers (**p4**, **p5**, **p7–p9**) account for up to 80 % of the total yield (Tables S2–S7) if the system behaves statistically, with significant fractions of xylene isomers (**p1**, **p2**) of up to 15 % being also produced.

### 1-Propynyl/1,3-Pentadiene System

The computations reveal that the outcome of the bimolecular reaction of the 1-propynyl radical with 1,3-pentadiene is quite distinct from that with isoprene. Overall, 10 reaction intermediates (**i20–i29**) were identified which are connected through 16 transition states. In detail, the 1-propynyl radical can add barrierlessly to any of the four carbon atoms of the  $\text{C1}=\text{C2}$  and  $\text{C3}=\text{C4}$  double bonds (Figure 4). Addition of 1-propynyl to  $\text{C2}$  or  $\text{C3}$  generates  $\text{sp}^3$ -hybridized carbon atom centered intermediates **i20** or **i24**. These structures can isomerize through ring closure via cyclic intermediates **i21** and **i25** followed by ring opening to allyl-type resonantly stabilized radicals **i22** and **i26**; these intermediates can also be accessed through the 1-propynyl radical addition to  $\text{C1}$  and  $\text{C4}$  of 1,3-pentadiene. Eventually, complexes **i22** and **i26** isomerize to **i23** and **i27–i29**, respectively, ultimately under-

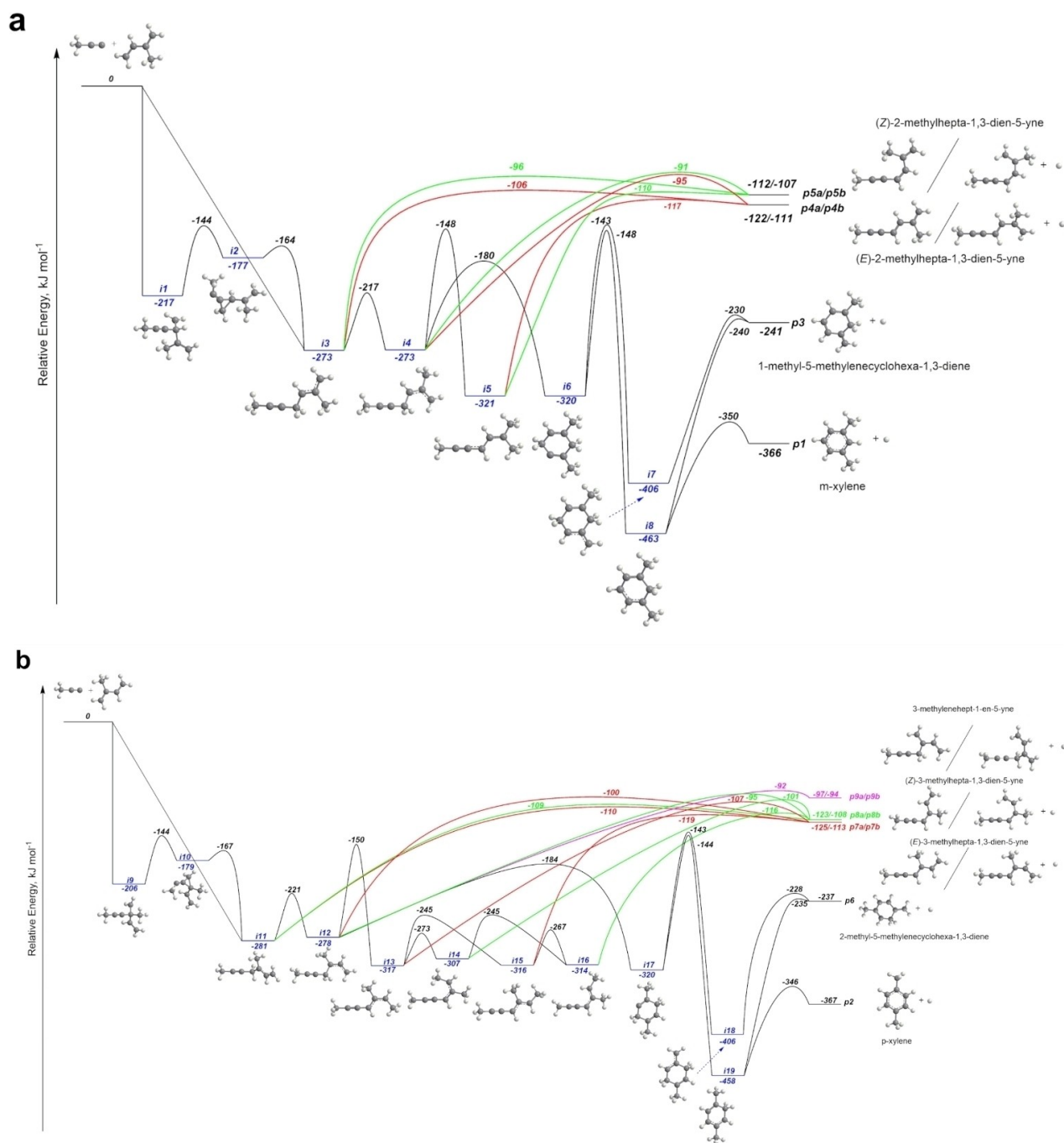


**Figure 3.** Potential energy surface for the bimolecular reaction of the 1-propynyl radical ( $\text{CH}_3\text{CC}$ ;  $X^2A_1$ ) with 2-methyl-1,3-butadiene ( $\text{CH}_2\text{C}(\text{CH}_3)\text{CHCH}_2$ ;  $X^1A'$ ) leading to  $\text{C}_8\text{H}_{10}$  plus H products calculated at the G3(MP2,CC)// $\omega$ B97X-D/6-311G(d,p) level of theory. Relative energies are given in  $\text{kJ mol}^{-1}$ ; a) addition to the C3=C4 bond; b) addition to the C1=C2 bond.

going unimolecular decomposition through methyl group loss forming **p10/p11** in overall exoergic reactions ( $-140$  to  $-156 \text{ kJ mol}^{-1}$ ). These energies correlate nicely with our experimental reaction exoergicities of  $145 \pm 39 \text{ kJ mol}^{-1}$  thus suggesting the formation of acyclic products **p10/p11** plus methyl radical under single collision conditions. These results are also in line with the statistical (RRKM) calculations revealing that methyl loss channels account for up to 90 % of the total product yield while atomic hydrogen

loss pathways originating from **i24** and **i26** lead only to minor  $\text{C}_8\text{H}_{10}$  products (Table S8, Figures S11–S13). Overall, two pairs of conformers for each (E)-hepta-1,3-dien-5-yne (**p10**) and (Z)-hepta-1,3-dien-5-yne (**p11**) prevail among the methyl elimination pathways (Figures 4). The distinct outcome of the reaction of the 1-propynyl radical with two  $\text{C}_5\text{H}_8$  isomers is likely a direct consequence of the molecular structure of the initial collision complexes formed in these processes. The eventually accessed substituted allylic radi-

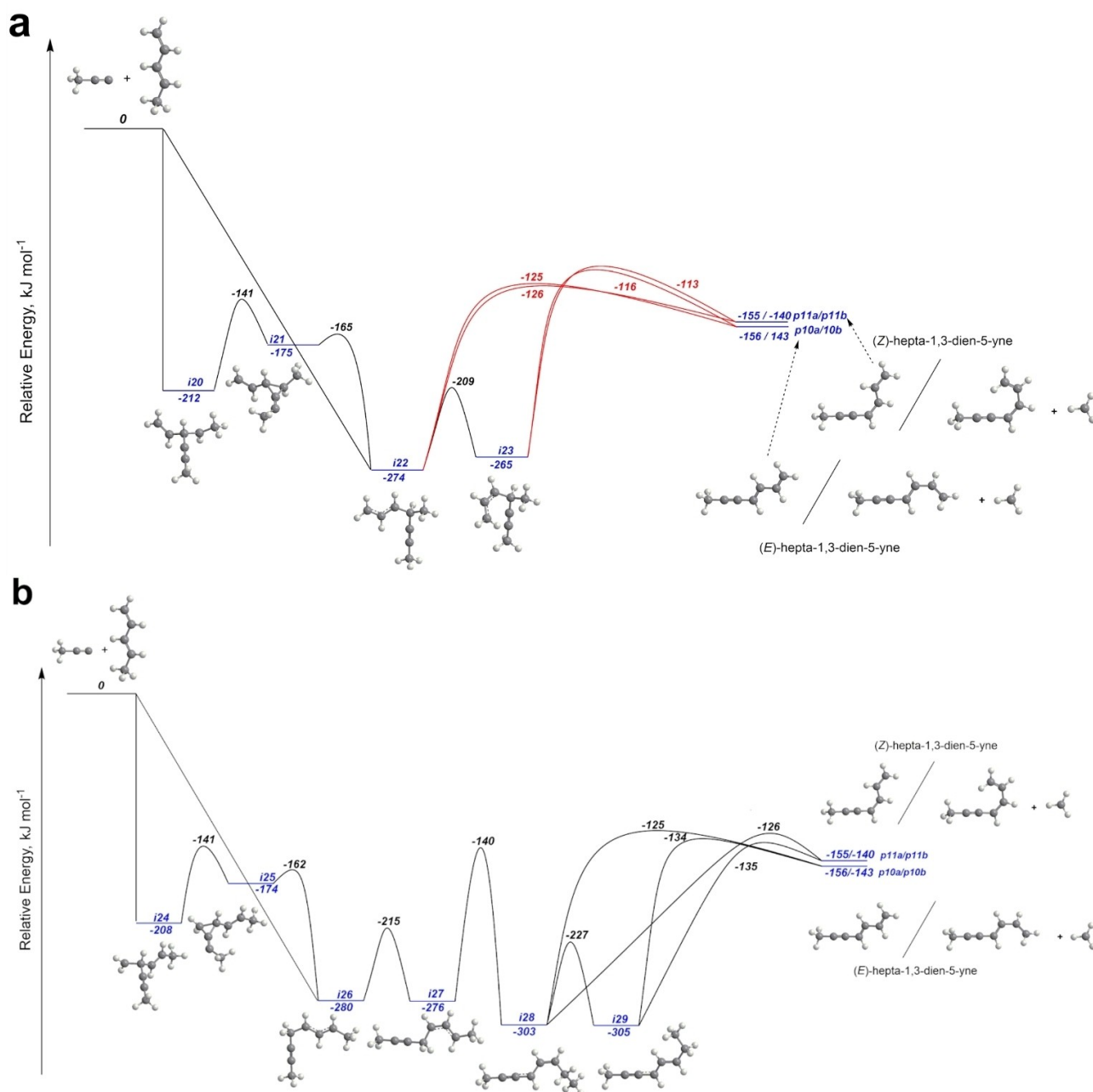


**Figure 4.** Potential energy surface for the bimolecular reaction of the 1-propynyl radical ( $\text{CH}_3\text{CC}$ ;  $X^2A_1$ ) with 1,3-pentadiene ( $\text{CH}_3\text{CHCHCHCH}_2$ ;  $X^1A'$ ) leading to  $\text{C}_7\text{H}_8$  isomers plus the methyl radical ( $\text{CH}_3$ ) calculated at the G3(MP2,CC)// $\omega$ B97X-D/6-311G(d,p) level of theory. Relative energies are given in  $\text{kJ mol}^{-1}$ . a) addition to the C3=C4 bond; b) addition to the C1=C2 bond.

cal restores the conjugated  $\pi$ -system by  $\beta$ -scission of the C–H or C–C bond. In the 1-propynyl/2-methyl-1,3-butadiene system (**i3**, **i11**) C–H bond rupture dominates; C–C bonds in the  $\beta$ -position are absent (**i11**) or the cleavage forms the thermodynamically less stable substituted allene moiety (**i3**) along with methyl. Considering the 1-propynyl / 1,3-pentadiene PES, all transition states associated with C–C bond ruptures are lower compared to those linked to C–H bond cleavage; this is indicative of dominating methyl loss channels as probed experimentally. The observed backward scattering can be best explained by dynamical prefer-

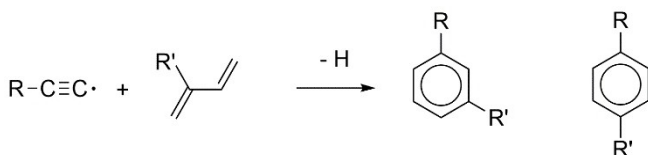
ence of the initial addition channel toward short-lived **i22**, while **i26** need to overcome a relatively high barrier of  $136 \text{ kJ mol}^{-1}$  toward to **i28** before emitting  $\text{CH}_3$ , which would result in a forward-backward scattering. Inspecting the natural charges in Table S11, the charge on the C5 atom (methyl group) is higher compared to all other C atoms ( $-0.60$ ). So the electrophilic radical center of  $\text{CH}_3\text{CC}$  may be attracted by the high electron density in the C1–C5 region of 1,3-pentadiene preferably adding to C1 to form **i22**. The steric hindrance can be upset by the strong attractive potential due to the high electron density. Overall,

this picture nicely accounts for the fast methyl loss channel in the 1-propynyl / 1,3-pentadiene system.

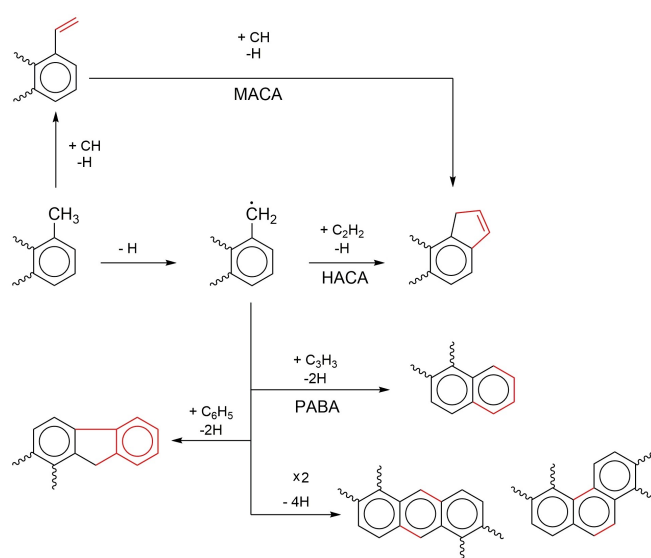
## Conclusion

Our combined experimental and computational study demonstrates a gas phase preparation of two xylene isomers - *m*-xylene (**p1**) and *p*-xylene (**p2**)—from two acyclic precursors, the 1-propynyl radical and 2-methyl-1,3-butadiene (isoprene), eventually functionalizing the benzene ring with two methyl groups via a single collision event. The reaction dynamics are driven by barrierless additions of the 1-propynyl radical to the diene moiety of 2-methyl-1,3-butadiene followed by extensive isomerization via, e.g., hydrogen shifts and ring closure prior to unimolecular decomposition via atomic hydrogen loss accompanied by aromatization in an overall exoergic reaction. Since all barriers to isomerization and product formation are located well below the energy of the separated reactants, the reaction of the 1-propynyl radical and 2-methyl-1,3-butadiene can prepare xylenes not only in high-temperature environments such as in combustion flames and around circumstellar envelopes of carbon-rich Asymptotic Giant Branch (AGB) stars, but also in low temperature cold molecular clouds (10 K) and in hydrocarbon-rich atmospheres of planets and their moons such as Triton and Titan. These studies also highlight the necessity of isomer-selective reaction dynamics studies since a switch of the methyl group from the C2 (in isoprene) to the C1 position (in 1,3-pentadiene) has a dramatic effect on the outcome of the reaction not only by de-facto preventing aromatization, but also in opening the methyl loss exit channels. In high temperature combustion and circumstellar environments, successive hydrogen atom assisted isomerization processes may also convert acyclic reaction products such as **p4**, **p5**, and **p7–p9** to xylenes thus amplifying the overall conversion of 1-propynyl radical into aromatic structures through its addition to the diene moiety of 2-methyl-1,3-butadiene.

A substitution of either methyl group in the 1-propynyl radical or in the closed shell 2-methyl-1,3-butadiene reactant by an alkyl group is further predicted to lead to preparation of more complex, disubstituted benzenes beyond xylenes in the gas phase (Scheme 2) thus affording a pathway to a versatile preparation of complex, aromatic organics even at ultralow temperatures of the deep space. These pathways may account for the high *meta/para* to *ortho* ratio of xylenes detected in the Orgueil (CI1) and Murchison (CM2) carbonaceous chondrites<sup>[6,7]</sup> and diethylbenzene in the coma



**Scheme 2.** Barrierless synthesis of disubstituted benzenes in reactions of alkylated ethynyl radicals with C2-substituted dienes.



**Scheme 3.** Fundamental mass-growth pathways of methyl substituted PAHs via annulation of five- and six-membered rings, radical self-recombination, and preparation of fluorene moieties.

of comet 67P/Churyumov-Gerasimenko.<sup>[37]</sup> These alkyl substituted aromatic molecules play a fundamental role in complex molecular mass growth processes as exemplified for methyl substituted benzene moieties (Scheme 3). Hydrogen abstraction can form the benzyloxy moiety involved in the Hydrogen Abstraction–C<sub>2</sub>H<sub>2</sub> (acetylene) Addition (HACA) pathway,<sup>[49–52]</sup> in the Propargyl Addition–BenzAnnulation (PABA) mechanism,<sup>[53]</sup> and self-recombination<sup>[54]</sup> yielding, e.g., annulated five- and six-membered rings along with fluorene moieties<sup>[55]</sup> thus highlighting the significance of alkyl-substituted-benzene moieties in the aromatic universe we live in.

## Supporting Information

The authors have cited additional references within the Supporting Information.<sup>[56–68]</sup>

## Acknowledgements

This work was supported by the U.S. Department of Energy, Basic Energy Sciences, by grant no. DE-FG02-03ER15411 to the University of Hawaii at Manoa and by grant no. DE-FG02-04ER15570 to the Florida International University.

## Conflict of Interest

The authors declare no conflict of interest.

## Data Availability Statement

The data that support the findings of this study are available from the corresponding author upon reasonable request.

**Keywords:** Gas-Phase Reactions · Propynyl · Reaction Mechanisms · Stereochemistry · Xylene

- [1] A. Cahours, *Compt. Rendus* **1850**, *30*, 319–323.
- [2] G. R. Galimova, I. A. Medvedkov, A. M. Mebel, *J. Phys. Chem. A* **2022**, *126*, 1233–1244.
- [3] A. Matsugi, A. Miyoshi, *Chem. Phys. Lett.* **2012**, *521*, 26–30.
- [4] G. Da Silva, E. E. Moore, J. W. Bozzelli, *J. Phys. Chem. A* **2009**, *113*, 10264–10278.
- [5] G. D. J. Guerrero Peña, M. M. Alrefaai, S. Y. Yang, A. Raj, J. L. Brito, S. Stephen, T. Anjana, V. Pillai, A. Al Shoaibi, S. H. Chung, *Combust. Flame* **2016**, *172*, 1–12.
- [6] M. A. Sephton, in *Treatise on Geochemistry*, Elsevier, Amsterdam, **2014**, pp. 1–31.
- [7] M. A. Sephton, *Geochim. Cosmochim. Acta* **2013**, *107*, 231–241.
- [8] M. Bohnet, *Ullmann's Encyclopedia of Industrial Chemistry*, Wiley-VCH, Weinheim, **2003**.
- [9] P. Hemberger, A. J. Trevitt, T. Gerber, E. Ross, G. Da Silva, *J. Phys. Chem. A* **2014**, *118*, 3593–3604.
- [10] F. Hirsch, M. Flock, I. Fischer, S. Bakels, A. M. Rijs, *J. Phys. Chem. A* **2019**, *123*, 9573–9578.
- [11] R. Bruckner, P. Wender, *Organic Mechanisms: Reactions, Stereochemistry and Synthesis*, Springer, Berlin, **2010**.
- [12] R. Taylor, *Electrophilic Aromatic Substitution*, Wiley, Chichester, New York, **1990**.
- [13] V. V. Kislov, A. M. Mebel, *J. Phys. Chem. A* **2007**, *111*, 3922–3931.
- [14] M. A. Oehlschlaeger, D. F. Davidson, R. K. Hanson, *J. Phys. Chem. A* **2006**, *110*, 9867–9873.
- [15] S.-H. Li, J.-J. Guo, R. Li, F. Wang, X.-Y. Li, *J. Phys. Chem. A* **2016**, *120*, 3424–3432.
- [16] R. Fröchtenicht, *J. Chem. Phys.* **1995**, *102*, 4850–4859.
- [17] X.-S. Xue, P. Ji, B. Zhou, J.-P. Cheng, *Chem. Rev.* **2017**, *117*, 8622–8648.
- [18] I. Da Costa, R. A. Eng, A. Gebert, H. Hippler, *Proc. Combust. Inst.* **2000**, *28*, 1537–1543.
- [19] A. M. Mebel, Y. Georgievskii, A. W. Jasper, S. J. Klippenstein, *Faraday Discuss.* **2017**, *195*, 637–670.
- [20] D. S. N. Parker, Ralf I. Kaiser, O. Kostko, M. Ahmed, *ChemPhysChem* **2015**, *16*, 2091–2093.
- [21] L. Zhao, M. B. Prendergast, R. I. Kaiser, B. Xu, W. Lu, U. Ablikim, M. Ahmed, A. D. Oleinikov, V. N. Azyazov, A. M. Mebel, A. H. Howlader, S. F. Wnuk, *ChemPhysChem* **2019**, *20*, 1437–1447.
- [22] A. M. Mebel, R. I. Kaiser, *Int. Rev. Phys. Chem.* **2015**, *34*, 461–514.
- [23] R. I. Kaiser, N. Hansen, *J. Phys. Chem. A* **2021**, *125*, 3826–3840.
- [24] R. I. Kaiser, D. S. N. Parker, A. M. Mebel, *Annu. Rev. Phys. Chem.* **2015**, *66*, 43–67.
- [25] K. O. Johansson, M. P. Head-Gordon, P. E. Schrader, K. R. Wilson, H. A. Michelsen, *Science* **2018**, *361*, 997–1000.
- [26] M. Thomson, T. Mitra, *Science* **2018**, *361*, 978–979.
- [27] L. Lai, W. H. Green, *J. Phys. Chem. A* **2019**, *123*, 3176–3184.
- [28] A. M. Thomas, L. Zhao, C. He, A. M. Mebel, R. I. Kaiser, *J. Phys. Chem. A* **2018**, *122*, 6663–6672.
- [29] A. M. Thomas, C. He, L. Zhao, G. R. Galimova, A. M. Mebel, R. I. Kaiser, *J. Phys. Chem. A* **2019**, *123*, 4104–4118.
- [30] C. He, L. Zhao, A. M. Thomas, A. N. Morozov, A. M. Mebel, R. I. Kaiser, *J. Phys. Chem. A* **2019**, *123*, 5446–5462.
- [31] C. He, L. Zhao, A. M. Thomas, G. R. Galimova, A. M. Mebel, R. I. Kaiser, *Phys. Chem. Chem. Phys.* **2019**, *21*, 22308–22319.
- [32] A. M. Thomas, S. Doddipatla, R. I. Kaiser, G. R. Galimova, A. M. Mebel, *Sci. Rep.* **2019**, *9*, 17595.
- [33] I. A. Medvedkov, A. A. Nikolayev, C. He, Z. Yang, A. M. Mebel, R. I. Kaiser, *Mol. Phys.* **2023**, e2234509.
- [34] S. Doddipatla, G. R. Galimova, H. Wei, A. M. Thomas, C. He, Z. Yang, A. N. Morozov, C. N. Shingledecker, A. M. Mebel, R. I. Kaiser, *Sci. Adv.* **2021**, *7*, eabd4044.
- [35] B. B. Kirk, J. D. Savee, A. J. Trevitt, D. L. Osborn, K. R. Wilson, *Phys. Chem. Chem. Phys.* **2015**, *17*, 20754–20764.
- [36] A. M. Burkhardt, K. Long Kelvin Lee, P. Bryan Changala, C. N. Shingledecker, I. R. Cooke, R. A. Loomis, H. Wei, S. B. Charnley, E. Herbst, M. C. McCarthy, B. A. McGuire, *ApJL* **2021**, *913*, L18.
- [37] N. Hänni, K. Altwegg, M. Combi, S. A. Fuselier, J. De Keyser, M. Rubin, S. F. Wampfler, *Nat. Commun.* **2022**, *13*, 3639.
- [38] M. H. Studier, R. Hayatsu, E. Anders, *Geochim. Cosmochim. Acta* **1972**, *36*, 189–215.
- [39] R. D. Levine, *Molecular Reaction Dynamics*, Cambridge University Press, Cambridge, **2009**.
- [40] Y. T. Lee, *Angew. Chem. Int. Ed. Engl.* **1987**, *26*, 939–951.
- [41] D. R. Herschbach, *Angew. Chem. Int. Ed. Engl.* **1987**, *26*, 1221–1243.
- [42] R. I. Kaiser, *Chem. Rev.* **2002**, *102*, 1309–1358.
- [43] R. I. Kaiser, P. Maksyutenko, C. Ennis, F. Zhang, X. Gu, S. P. Krishtal, A. M. Mebel, O. Kostko, M. Ahmed, *Faraday Discuss.* **2010**, *147*, 429–478.
- [44] W. B. Miller, S. A. Safron, D. R. Herschbach, *J. Chem. Phys.* **1972**, *56*, 3581–3592.
- [45] M. F. Vernon, *Molecular Beam Scattering*, Ph.D. Dissertation, University of California, **1983**.
- [46] P. S. Weiss, *Reaction Dynamics of Electronically Excited Alkali Atoms with Simple Molecules*, Ph.D. Dissertation, University of California, **1986**.
- [47] L. A. Curtiss, K. Raghavachari, P. C. Redfern, A. G. Baboul, J. A. Pople, *Chem. Phys. Lett.* **1999**, *314*, 101–107.
- [48] Y. Minenkov, Å. Singstad, G. Occhipinti, V. R. Jensen, *Dalton Trans.* **2012**, *41*, 5526.
- [49] D. S. N. Parker, R. I. Kaiser, T. P. Troy, M. Ahmed, *Angew. Chem. Int. Ed.* **2014**, *53*, 7740–7744.
- [50] T. Yang, T. P. Troy, B. Xu, O. Kostko, M. Ahmed, A. M. Mebel, R. I. Kaiser, *Angew. Chem. Int. Ed.* **2016**, *55*, 14983–14987.
- [51] T. Yang, R. I. Kaiser, T. P. Troy, B. Xu, O. Kostko, M. Ahmed, A. M. Mebel, M. V. Zagidullin, V. N. Azyazov, *Angew. Chem. Int. Ed.* **2017**, *56*, 4515–4519.
- [52] L. Zhao, R. I. Kaiser, B. Xu, U. Ablikim, M. Ahmed, D. Joshi, G. Veber, F. R. Fischer, A. M. Mebel, *Nat. Astron.* **2018**, *2*, 413–419.
- [53] C. He, R. I. Kaiser, W. Lu, M. Ahmed, V. S. Krasnoukhov, P. S. Pivovarov, M. V. Zagidullin, V. N. Azyazov, A. N. Morozov, A. M. Mebel, *Chem. Sci.* **2023**, *14*, 5369–5378.
- [54] R. I. Kaiser, L. Zhao, W. Lu, M. Ahmed, V. S. Krasnoukhov, V. N. Azyazov, A. M. Mebel, *Nat. Commun.* **2022**, *13*, 786.
- [55] C. He, R. I. Kaiser, W. Lu, M. Ahmed, P. S. Pivovarov, O. V. Kuznetsov, M. V. Zagidullin, A. M. Mebel, *Angew. Chem.* **2023**, *135*, e202216972.
- [56] Y. Guo, X. Gu, E. Kawamura, R. I. Kaiser, *Rev. Sci. Instrum.* **2006**, *77*, 034701.
- [57] D. Proch, T. Trickl, *Rev. Sci. Instrum.* **1989**, *60*, 713–716.
- [58] D. Trogolo, A. Maranzana, G. Ghigo, G. Tonachini, *Combust. Flame* **2016**, *168*, 331–341.
- [59] N. R. Daly, *Rev. Sci. Instrum.* **1960**, *31*, 264–267.

- [60] J.-D. Chai, M. Head-Gordon, *Phys. Chem. Chem. Phys.* **2008**, *10*, 6615–6620.
- [61] L. A. Curtiss, K. Raghavachari, P. C. Redfern, V. Rassolov, J. A. Pople, *J. Chem. Phys.* **1998**, *109*, 7764–7776.
- [62] A. G. Baboul, L. A. Curtiss, P. C. Redfern, K. Raghavachari, *J. Chem. Phys.* **1999**, *110*, 7650–7657.
- [63] M. J. Frisch, G. W. Trucks, H. B. Schlegel, G. E. Scuseria, M. A. Robb, J. R. Cheeseman, G. Scalmani, V. Barone, B. Mennucci, G. A. Petersson, H. Nakatsuji, M. Caricato, X. Li, H. P. Hratchian, A. F. Izmaylov, J. Bloino, G. Zheng, J. L. Sonnenberg, M. Hada, M. Ehara, K. Toyota, R. Fukuda, J. Hasegawa, M. Ishida, T. Nakajima, Y. Honda, O. Kitao, H. Nakai, T. Vreven, J. A. Montgomery, J. E. Peralta, F. Ogliaro, M. Bearpark, J. J. Heyd, E. Brothers, K. N. Kudin, V. N. Staroverov, R. Kobayashi, J. Normand, K. Raghavachari, A. Rendell, J. C. Burant, S. S. Iyengar, J. Tomasi, M. Cossi, N. Rega, J. M. Millam, M. Klene, J. E. Knox, J. B. Cross, V. Bakken, C. Adamo, J. Jaramillo, R. Gomperts, R. E. Stratmann, O. Yazyev, A. J. Austin, R. Cammi, C. Pomelli, J. W. Ochterski, R. L. Martin, K. Morokuma, V. G. Zakrzewski, G. A. Voth, P. Salvador, J. J. Dannenberg, S. Dapprich, A. D. Daniels, Ö. Farkas, J. B. Foresman, J. V. Ortiz, J. Cioslowski, D. J. Fox, Gaussian 09, Revision D.1, Gaussian., Gaussian Inc.: Wallingford, CT, **2009**.
- [64] H.-J. Werner, P. J. Knowles, R. Lindh, F. R. Manby, M. Schütz, P. Celani, T. Korona, G. Rauhut, R. D. Amos, A. Bernhardsson, MOLPRO, Version 2015.1, A Package of Ab Initio Programs, University of Cardiff: Cardiff: UK, **2015**.
- [65] J. I. Steinfeld, J. S. Francisco, W. L. Hase, *Chemical Kinetics and Dynamics*, Pearson, Upper Saddle River, N.J., **1998**.
- [66] H. Eyring, S. H. Lin, S. M. Lin, *Basic Chemical Kinetics*, John Wiley And Sons, New York, **1980**.
- [67] P. J. Robinson, K. A. Holbrook, *Unimolecular Reactions*, John Wiley And Sons, New York, **1972**.
- [68] V. V. Kislov, T. L. Nguyen, A. M. Mebel, S. H. Lin, S. C. Smith, *J. Chem. Phys.* **2004**, *120*, 7008–7017.
- Manuscript received: October 9, 2023  
Accepted manuscript online: December 10, 2023  
Version of record online: December 20, 2023